

# Hybrid structures formed by homo- and heteroleptic aliphatic dicarboxylates of lead with 2-D inorganic connectivity

A. Thirumurugan, C.N.R. Rao\*

Chemistry and Physics of Materials Unit, Jawaharlal Nehru Centre for Advanced Scientific Research, Jakkur P.O., Bangalore 560064, India

Received 17 December 2007; received in revised form 12 February 2008; accepted 18 February 2008

Available online 29 February 2008

## Abstract

Three-dimensional homoleptic (single type of ligand) lead dicarboxylates with hybrid structures involving Pb–O–Pb linkages of the compositions,  $\text{Pb}(\text{C}_5\text{H}_6\text{O}_4)$ , **I**, and  $\text{Pb}(\text{C}_6\text{H}_8\text{O}_4)$ , **II** and **III**, have been synthesized and characterized. Three-dimensional heteroleptic (mixed ligands) lead dicarboxylates of the formulae,  $\text{Pb}_2(\text{C}_2\text{O}_4)(\text{C}_4\text{H}_4\text{O}_4)$ , **IV** and  $\text{Pb}_2(\text{C}_2\text{O}_4)(\text{C}_6\text{H}_8\text{O}_4)$ , **V**, with hybrid structures involving Pb–O–Pb linkages have also been prepared and characterized along with a novel two-dimensional lead nitrate-oxalate of the composition,  $(\text{OPb}_2)_2(\text{C}_2\text{O}_4)(\text{NO}_3)_2$ , **VI**. In all these dicarboxylates, there is two-dimensional inorganic connectivity and the lead (II) cation has hemi- or holo-directed coordination geometry. Depending upon the torsional angle and the coordination mode of the dicarboxylate anions as well as the geometry of the lead (II) cations, these hybrid compounds exhibit two types of two-dimensional inorganic connectivities.

© 2008 Elsevier Inc. All rights reserved.

**Keywords:** Inorganic–organic hybrid frameworks; Aliphatic dicarboxylates; Mixed ligands; Nitrate; Lead

## 1. Introduction

Metal carboxylates with different framework structures are being investigated in-depth in the last few years [1–4]. Some of the carboxylates possess interesting properties as exemplified by the metal-organic frameworks synthesized by Yaghi et al. [5], which show excellent hydrogen sorption properties. Then, there are trinuclear chromium cluster-based benzene di- and tri-carboxylates synthesized by Férey et al. [6,7] which possess very large surface areas and unit cell volumes going up to  $700,000 \text{ \AA}^3$ . Of particular interest to us are the inorganic organic hybrid frameworks with infinite metal–oxygen–metal bonds. Hybrid metal carboxylates with interesting properties have been reported in the literature. Aliphatic dicarboxylic acids have been used as good linkers in the construction of hybrid compounds with interesting structures [8–16]. Recently [17], hybrid frameworks have been classified on the basis of the dimensionality ( $n$ ,  $m$ ) of the inorganic

( $I$ ) and organic ( $O$ ) connectivities, to define a characteristic  $I^n O^m$ . Hybrid structures with two-dimensional (2-D) inorganic connectivity ( $I^2$ ) are known in the literature [8,9,18–24]. There are very few mixed aliphatic dicarboxylates known today, the only examples, to our knowledge being the neodymium oxalate-glutarate [25],  $\text{Nd}_4(\text{H}_2\text{O})_2(\text{C}_5\text{H}_6\text{O}_4)_4(\text{C}_2\text{O}_4)_2$ , lanthanum oxalate-succinate [26],  $[\text{La}_2(\text{C}_2\text{O}_4)(\text{C}_4\text{H}_4\text{O}_4)_2(\text{H}_2\text{O})_4] \cdot 4\text{H}_2\text{O}$ , lanthanum oxalate-adipate [26],  $\text{La}_2(\text{C}_2\text{O}_4)_2(\text{C}_6\text{H}_8\text{O}_4)(\text{H}_2\text{O})_2$ , lanthanide oxalate-fumarate [27],  $[\text{La}_2(\text{C}_2\text{O}_4)(\text{C}_4\text{H}_2\text{O}_4)_2(\text{H}_2\text{O})_4] \cdot 4\text{H}_2\text{O}$  ( $Ln = \text{Eu}, \text{Tb}$ ). In this article, we describe the synthesis and structure of hybrid aliphatic dicarboxylates of lead with 2-D inorganic connectivities of the type  $I^2 O^m$  where  $m = 0$  or 1. The compounds synthesized and characterized by us include a glutarate,  $\text{Pb}(\text{C}_5\text{H}_6\text{O}_4)$ , **I**, and two adipates of the same formula,  $\text{Pb}(\text{C}_6\text{H}_8\text{O}_4)$ , **II**, and **III**, in addition to two mixed carboxylates, an oxalate-succinate,  $\text{Pb}_2(\text{C}_2\text{O}_4)(\text{C}_4\text{H}_4\text{O}_4)$ , **IV**, and an oxalate-adipate,  $\text{Pb}_2(\text{C}_2\text{O}_4)(\text{C}_6\text{H}_8\text{O}_4)$ , **V**. We also report a nitrate-oxalate,  $(\text{OPb}_2)_2(\text{C}_2\text{O}_4)(\text{NO}_3)_2$ , **VI**, where the nitrate and oxalate anions coordinate with the metal ion.

\*Corresponding author. Fax: +91 80 2208 2760.

E-mail address: [cnrrao@jncasr.ac.in](mailto:cnrrao@jncasr.ac.in) (C.N.R. Rao).

## 2. Experimental

### 2.1. Synthesis and characterization

#### 2.1.1. Materials and methods

Pb(NO<sub>3</sub>)<sub>2</sub> (Qualigens, India, 99%), oxalic acid dihydrate (C<sub>2</sub>H<sub>2</sub>O<sub>4</sub>·2H<sub>2</sub>O) (S.D. Fine, India, 99.5%), succinic acid (C<sub>4</sub>H<sub>6</sub>O<sub>4</sub>) (Qualigens, India, 99%), glutaric acid (C<sub>5</sub>H<sub>8</sub>O<sub>4</sub>) (Spectrochem, India, 99%), adipic acid (C<sub>6</sub>H<sub>10</sub>O<sub>4</sub>) (Merck, India, 99%), NaOH (Merck, India, 99%) of high purity and double distilled water were used for the synthesis.

The Pb aliphatic dicarboxylates **I–VI** were synthesized under hydrothermal conditions by heating the homogenized reaction mixtures in a 23 mL PTFE-lined bomb at the 180 °C temperature for 72 h under autogeneous pressure. The pH of the starting reaction mixture was generally in the range 5–6. The pH after the reaction did not show appreciable change. The products of the hydrothermal reactions were vacuum-filtered and dried under ambient conditions. The starting compositions for the different compounds synthesized by us are given in Table 1. All the compounds were obtained as single phase materials, except **III**, whose crystals were admixed with small quantities of lead succinate, Pb(C<sub>4</sub>H<sub>4</sub>O<sub>4</sub>) [28]. Attempts were made unsuccessfully to prepare **III** in pure form without the addition of succinic acid. The crystals of **I**, **II**, **IV**, **V** and **VI** were separated under a polarizing microscope and used for all the characterization. Other than the single-crystal X-ray diffraction (XRD), **III** could not be subjected to other methods of characterization due to the difficulty in separating the lead succinate impurity.

Elemental analyses were satisfactory. For **I**, (C<sub>5</sub>H<sub>6</sub>PbO<sub>4</sub>) calcd.: C, 17.79%; H, 1.78%. Found: C, 18.09%; H, 1.63%; For **II**, (C<sub>6</sub>H<sub>8</sub>PbO<sub>4</sub>) calcd.: C, 20.50%; H, 2.28%. Found: C, 21.06%; H, 2.15%. For **IV**, (C<sub>3</sub>H<sub>2</sub>PbO<sub>4</sub>) calcd.: C, 11.64%; H, 0.65%. Found: C, 11.92%; H, 0.87%. For **V**, (C<sub>4</sub>H<sub>4</sub>PbO<sub>4</sub>) calcd.: C, 14.85%; H, 1.24%. Found: C, 15.12%; H, 1.36%. For **VI**, (CNPb<sub>2</sub>O<sub>6</sub>) calcd.: C, 2.24%; N, 2.61%. Found: C, 2.36%; N, 2.84%.

Powder XRD patterns of the products were recorded using CuK $\alpha$  radiation (Rich-Seifert, 3000TT). The patterns agreed with those calculated for single crystal structure determination. Thermogravimetric analysis (TGA) was carried out (Metler-Toledo) in oxygen atmosphere (flow rate = 50 mL/min) in the temperature range 25–800 °C (heating rate = 5 °C/min).

Infrared (IR) spectra of KBr pellets of the compounds were recorded in the mid IR region (Bruker IFS-66v). All the compounds show characteristic bands of the functional groups [29–31]. The bands around 1600 and 1400 cm<sup>-1</sup> are assigned to the asymmetric ( $\nu_{as}$  C=O) and symmetric ( $\nu_s$  C=O) stretching of the carboxylate anion. The bands at 1285 ( $\nu_{as}$  N–O), 1017 ( $\nu_s$  N–O), 752 ( $\delta_{NO_3}$ ) in-plane and 817 cm<sup>-1</sup> ( $\delta_{NO_3}$ ) out-of-plane indicate the presence of the nitrate groups in **VI**.

Thermogravimetric analyses of the Pb dicarboxylates are as follows. All the compounds show single-step weight loss. For **I**, the weight loss of 34.36% (calcd. 33.80%) occurred in the 310–450 °C range. For **II**, the weight loss of 36.82% (calcd. 36.44%) occurred in the 295–440 °C range. For **IV**, the weight loss of 28.17% (calcd. 27.79%) occurred in the 300–450 °C range. For **V**, the weight loss of 31.33% (calcd. 30.92%) occurred in the 295–450 °C range. The total weight loss matches very well with the loss of CO<sub>2</sub> and H<sub>2</sub>O and the formation of PbO (PDF no. 00-004-0561) in all the cases. TGA could not be performed in **VI** due to the highly exothermic nature of the decomposition.

A suitable single crystal of each compound was carefully selected under a polarizing microscope and glued to a thin glass fiber. Crystal structure determination by XRD was performed on a Bruker–Nonius diffractometer with Kappa geometry attached with an APEX-II-CCD detector and a graphite monochromator for the X-ray source (MoK $\alpha$  radiation,  $\lambda$  = 0.71073 Å) operating at 50 kV and 30 mA. An empirical absorption correction based on symmetry equivalent reflections was applied using the SADABS program [32]. The structure was solved and refined using SHELXTL-PLUS suite of programs [33]. For the final

Table 1  
Synthetic conditions for compounds **I–VI**

Compound no.	Formula	Composition (mole ratio)				Yield based on lead (%)	
		Pb(NO <sub>3</sub> ) <sub>2</sub>	Dicarboxylic acid		NaOH (5 M soln.)		Water
<b>I</b>	Pb(C <sub>5</sub> H <sub>6</sub> O <sub>4</sub> )	(0.333 g)1	Glutaric acid (0.267 g) 2		(0.5 mL) 2.5	(5 mL) 278	54
<b>II</b>	Pb(C <sub>6</sub> H <sub>8</sub> O <sub>4</sub> )	(0.333 g)1	Adipic acid (0.295 g) 2		(0.6 mL) 3	(5 mL) 278	61
<b>III</b>	Pb(C <sub>6</sub> H <sub>8</sub> O <sub>4</sub> )	(0.333 g)1	Succinic acid (0.0596 g) 0.5	Adipic acid (0.295 g) 2	(0.5 mL) 2.5	(5 mL) 278	–
<b>IV</b>	Pb <sub>2</sub> (C <sub>2</sub> O <sub>4</sub> )(C <sub>4</sub> H <sub>4</sub> O <sub>4</sub> )	(0.333 g)1	Oxalic acid·2H <sub>2</sub> O (0.127 g)1	Succinic acid (0.238 g) 2	(1.0 mL) 5	(5 mL) 278	67
<b>V</b>	Pb <sub>2</sub> (C <sub>2</sub> O <sub>4</sub> )(C <sub>6</sub> H <sub>8</sub> O <sub>4</sub> )	(0.333 g)1	Oxalic acid·2H <sub>2</sub> O (0.127 g)1	Adipic acid (0.295 g) 2	(0.8 mL) 4	(5 mL) 278	64
<b>VI</b>	(OPb <sub>2</sub> ) <sub>2</sub> (C <sub>2</sub> O <sub>4</sub> )(NO <sub>3</sub> ) <sub>2</sub>	(0.333 g)1	Oxalic acid·2H <sub>2</sub> O (0.19 g) 1.5		(0.6 mL) 3	(5 mL) 278	56

refinement the hydrogen atoms were placed geometrically and held in the riding mode. Final refinement included atomic positions for all the atoms, anisotropic thermal parameters for all the non-hydrogen atoms and isotropic thermal parameters for the hydrogen atoms. All the hydrogen atoms were included in the final refinement. Details of the structure solution and final refinements for compounds I–VI are given in Tables 2 and 3.

### 3. Results and discussion

We have synthesized three homoleptic (single type of ligand) hybrid metal dicarboxylates of the composition,  $\text{Pb}(\text{C}_5\text{H}_6\text{O}_4)$ , **I**, and two polymorphs of  $\text{Pb}(\text{C}_6\text{H}_8\text{O}_4)$ , **II** and **III**, involving the coordination of glutarate and adipate anions to the Pb(II) cation, in addition to two heteroleptic (mixed) carboxylates of lead,  $\text{Pb}_2(\text{C}_2\text{O}_4)(\text{C}_4\text{H}_4\text{O}_4)$ , **IV**, and  $\text{Pb}_2(\text{C}_2\text{O}_4)(\text{C}_6\text{H}_8\text{O}_4)$ , **V**, formed by oxalate and succinate or adipate. We have also prepared an unusual dicarboxylate,  $(\text{OPb}_2)_2(\text{C}_2\text{O}_4)(\text{NO}_3)_2$ , **VI**, where the nitrate ion coordinates with the metal ion along with the oxalate anion. In what follows, we discuss the structures of I–VI.

The glutarate,  $\text{Pb}(\text{C}_5\text{H}_6\text{O}_4)$ , **I**, has a three-dimensional (3-D) structure with an asymmetric unit of nine non-hydrogen atoms (Fig. 1a). The asymmetric unit contains a crystallographically distinct  $\text{Pb}^{2+}$  ion and half of the glutarate anion where all the atoms have a 0.5 occupancy except O(3) which sits at the 4f position. The glutarate anion with a molecular mirror plane exhibits a coordina-

Table 2  
Crystal data and structure refinement parameters for I–III

Structure parameter	I	II	III
Empirical formula	$\text{C}_5\text{H}_6\text{PbO}_4$	$\text{C}_6\text{H}_8\text{PbO}_4$	$\text{C}_6\text{H}_8\text{PbO}_4$
Formula weight	337.29	351.31	351.31
Crystal system	Monoclinic	Monoclinic	Monoclinic
Space group	$P2_1/m$ (no. 11)	$P2_1/c$ (no. 14)	$P2_1/c$ (no. 14)
$a$ ( $\text{\AA}^{-1}$ )	4.7454(1)	7.2156(1)	20.5361(7)
$b$ ( $\text{\AA}^{-1}$ )	7.2032(1)	4.7367(1)	5.0737(2)
$c$ ( $\text{\AA}^{-1}$ )	9.6750(1)	21.9305(4)	7.0706(2)
$\beta$ ( $\text{deg}^{-1}$ )	93.164(1)	90.417(1)	92.147(1)
$V$ ( $\text{\AA}^{-3}$ )	330.21(1)	749.52(2)	736.20(4)
$Z$	2	4	4
$D(\text{calcd.})$ ( $\text{g/cm}^3$ )	3.392	3.113	3.170
$\mu$ ( $\text{mm}^{-1}$ )	25.494	22.470	22.876
Total data collected	2170	4825	7160
Unique data	607	1387	1269
Observed data	591	1307	1221
$[I > 2\sigma(I)]$			
$R_{\text{merg}}$	0.0277	0.0349	0.0276
Goodness of fit	1.082	1.037	1.133
$R$ indexes	$R_1 = 0.0396^a$	$R_1 = 0.0182^a$	$R_1 = 0.0450^a$
$[I > 2\sigma(I)]$	$wR_2 = 0.0897^b$	$wR_2 = 0.0416^b$	$wR_2 = 0.1080^b$
$R$ indexes	$R_1 = 0.0401^a$	$R_1 = 0.0200^a$	$R_1 = 0.00459^a$
[All data]	$wR_2 = 0.0906^b$	$wR_2 = 0.0424^b$	$wR_2 = 0.1106^b$

$$^a R_1 = \sum ||F_o| - |F_c|| / \sum |F_o|.$$

$$^b wR_2 = \{ \sum [w(F_o^2 - F_c^2)^2] / \sum [w(F_o^2)] \}^{1/2}. w = 1 / [\sigma^2(F_o)^2 + (aP)^2 + bP], P = [\max.(F_o^2, 0) + 2(F_c^2)] / 3, \text{ where } a = 0.0773, b = 0 \text{ for I, } a = 0.0183, b = 0.3362 \text{ for II and } a = 0.0828, b = 0.7243 \text{ for III.}$$

Table 3  
Crystal data and structure refinement parameters for IV–VI

Structure parameter	IV	V	VI
Empirical formula	$\text{C}_3\text{H}_2\text{PbO}_4$	$\text{C}_4\text{H}_4\text{PbO}_4$	$\text{CNPb}_2\text{O}_6$
Formula weight	309.24	323.27	536.40
Crystal system	Monoclinic	Monoclinic	Monoclinic
Space group	$P2_1/c$ (no. 14)	$P2_1/m$ (no. 11)	$P2_1/c$ (no. 14)
$a$ ( $\text{\AA}^{-1}$ )	12.6902(5)	15.1995(8)	11.8682(3)
$b$ ( $\text{\AA}$ )	5.2086(2)	5.1505(3)	5.2501(1)
$c$ ( $\text{\AA}^{-1}$ )	6.9389(2)	7.0289(4)	9.0989(2)
$\beta$ ( $\text{deg}^{-1}$ )	100.507(2)	98.072(3)	96.741(2)
$v$ ( $\text{\AA}^{-3}$ )	450.96(3)	544.81(5)	563.03(2)
$Z$	4	4	4
$D(\text{calcd.})$ ( $\text{g/cm}^3$ )	4.555	3.941	6.328
$\mu$ ( $\text{mm}^{-1}$ )	37.312	30.894	59.696
Total data collected	7700	11864	3355
Unique data	720	965	1007
Observed data			
$[I > 2\sigma(I)]$	710	939	952
$R_{\text{merg}}$	0.0236	0.0183	0.0915
Goodness of fit	1.136	1.214	1.058
$R$ indexes	$R_1 = 0.0428^a$	$R_1 = 0.0305^a$	$R_1 = 0.0528^a$
$[I > 2\sigma(I)]$	$wR_2 = 0.1012^b$	$wR_2 = 0.0764^b$	$wR_2 = 0.1187^b$
$R$ indexes	$R_1 = 0.0430^a$	$R_1 = 0.0310^a$	$R_1 = 0.0548^a$
[All data]	$wR_2 = 0.1014^b$	$wR_2 = 0.0768^b$	$wR_2 = 0.1211^b$

$$^a R_1 = \sum ||F_o| - |F_c|| / \sum |F_o|.$$

$$^b wR_2 = \{ \sum [w(F_o^2 - F_c^2)^2] / \sum [w(F_o^2)] \}^{1/2}. w = 1 / [\sigma^2(F_o)^2 + (aP)^2 + bP], P = [\max.(F_o^2, 0) + 2(F_c^2)] / 3, \text{ where } a = 0.0838, b = 0.3233 \text{ for IV, } a = 0.00467, b = 1.7204 \text{ for V and } a = 0.0764, b = 10.0162 \text{ for VI.}$$

tion mode with (1222) connectivity (for description of connectivity see [34]) with the torsional angle of  $95.01(2)^\circ$  (Fig. 1b). The Pb atom is hemi-directed (where the ligating atoms bind only from one side of the polyhedra and form a hemisphere like geometry, due to the stereochemically active lone pair of electrons in the cation) and seven-coordinated by oxygen atoms ( $\text{PbO}_7$ ) from five different glutarate anions. Six of the oxygens have  $\mu_3$  connections linking each Pb with four other Pb atoms. Thus, a  $\text{PbO}_7$  polyhedron shares its two corners with two different  $\text{PbO}_7$  polyhedra and two edges with two other  $\text{PbO}_7$  forming an infinite 2-D Pb–O–Pb layer of the  $I^2O^0$  type, with a (4,4) net topology (Fig. 1c). This layer can be viewed as chains of edge shared  $\text{PbO}_7$  polyhedra connected through the corners of  $\text{PbO}_7$  polyhedra of the adjacent chains. The layers get further connected to each other through glutarate anions into a 3-D structure of the  $I^2O^1$  type (Fig. 1d). The Pb–O bond lengths are in the 2.399–2.853  $\text{\AA}$  range.

The adipate,  $\text{Pb}(\text{C}_6\text{H}_8\text{O}_4)$ , **II**, has a 3-D structure similar to **I**, with an asymmetric unit of 11 non-hydrogen atoms (Fig. 2a). The asymmetric unit contains a crystallographically distinct  $\text{Pb}^{2+}$  ion and one adipate anion. The adipate anion exhibits a coordination mode with (1222) connectivity and a torsional angle of  $108.19(3)^\circ$ . The Pb atom is hemi-directed and seven-coordinated by oxygen atoms from five different adipate anions. Six of the oxygens have  $\mu_3$  connections linking each Pb with four other Pb atoms giving rise to an infinite 2-D Pb–O–Pb layer of the  $I^2O^0$  type, with a (4,4) net topology just as in **I** (Fig. 1c) and a

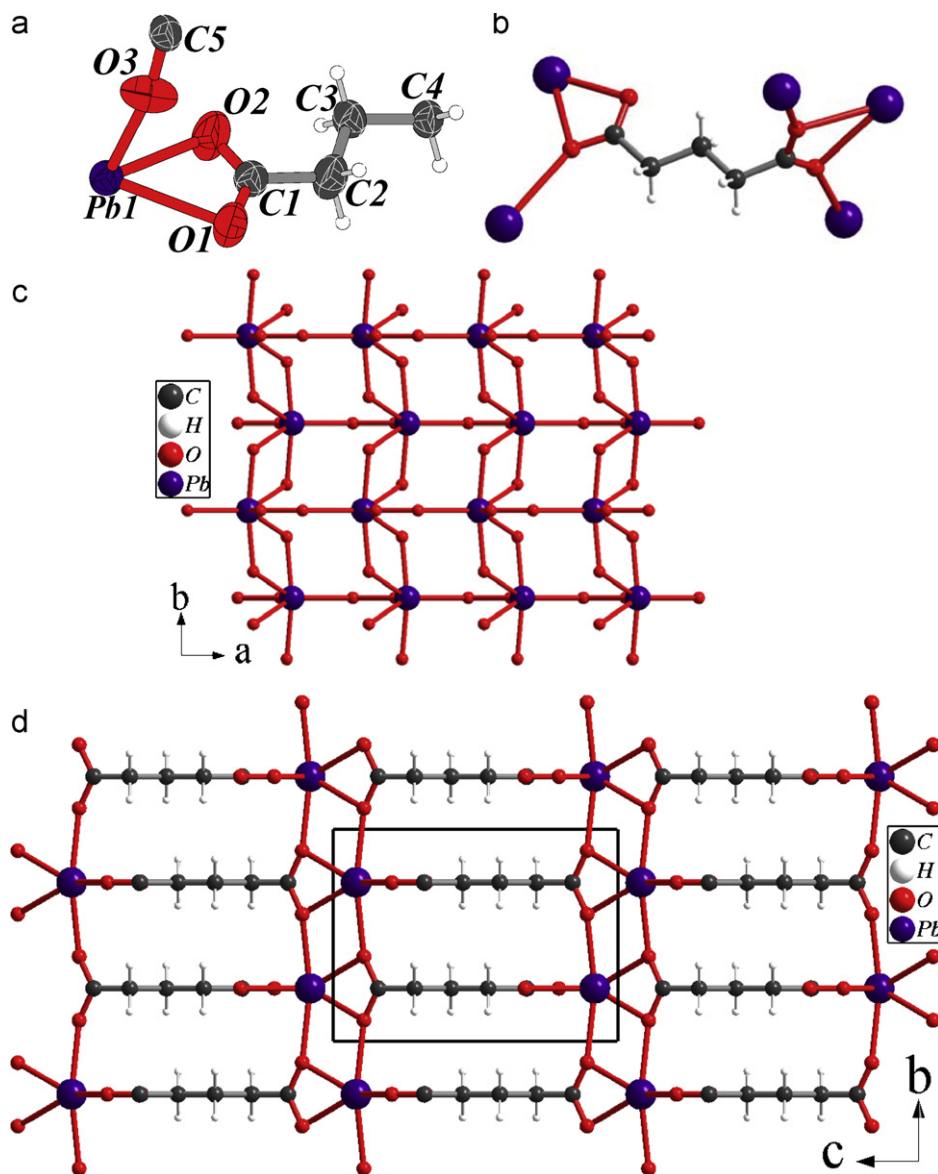


Fig. 1. (a) ORTEP plot of  $\text{Pb}(\text{C}_5\text{H}_6\text{O}_4)$ , **I** (thermal ellipsoids are shown at 50% probability), (b) coordination mode of the glutarate moiety in **I**, (c) view of the inorganic layer with the infinite  $\text{Pb-O-Pb}$  linkages of the  $P^2O^0$  type in **I** and (d) the 3-D structure of **I** viewed along the  $a$ -axis.

3-D structure of the  $P^2O^1$  type through adipate connectivity (Fig. 2b). The  $\text{Pb-O}$  bond lengths in **II** are in the 2.398–2.864 Å range.

Another adipate,  $\text{Pb}(\text{C}_6\text{H}_8\text{O}_4)$ , **III**, is a polymorph of **II**, also has a 3-D structure with an asymmetric unit of 11 non-hydrogen atoms (Fig. 3a). The asymmetric unit contains a crystallographically distinct  $\text{Pb}^{2+}$  ion and an adipate anion. The adipate anion exhibits a coordination mode with (1212) connectivity and a torsional angle of  $0^\circ$  (Fig. 3b). The  $\text{Pb}$  atom is holo-directed (where the ligating atoms bind from all the sides of the polyhedra) and seven-coordinated by oxygen atoms from six different adipate anions. Six of the oxygens have  $\mu_3$  connections linking each  $\text{Pb}$  atom with four other  $\text{Pb}$  atoms. Thus, a  $\text{PbO}_7$  polyhedron shares its two corners with two  $\text{PbO}_7$  polyhedra and two of its edges with other two  $\text{PbO}_7$  forming an infinite 2-D  $\text{Pb-O-Pb}$  layer of the  $P^2O^0$  type,

with a (4,4) net topology different from compounds **I** and **II** (Fig. 3c). This layer contains of  $\text{PbO}_7$  polyhedra connected to each other through edges and corners. The layers are further connected to each other through the adipate anions into a 3-D structure of the  $P^2O^1$  type (Fig. 3d). The  $\text{Pb-O}$  bond lengths are in the 2.386–2.925 Å range. Compounds **I** and **II** provide a nice example for the structural polymorphism with same chemical formula but with different 2-D inorganic connectivity.

The oxalate-succinate,  $\text{Pb}_2(\text{C}_2\text{O}_4)(\text{C}_4\text{H}_4\text{O}_4)$ , **IV**, has a 3-D structure with an asymmetric unit of 8 non-hydrogen atoms (Fig. 4a). The asymmetric unit contains a crystallographically distinct  $\text{Pb}^{2+}$  ion, one half of the oxalate and one half of the succinate anions. The oxalate and succinate anions exhibit coordination modes with (2222) and (1121) connectivities, respectively, both with  $0^\circ$  torsional angle (Figs. 4b and c). The  $\text{Pb}$  atom is holo-directed and

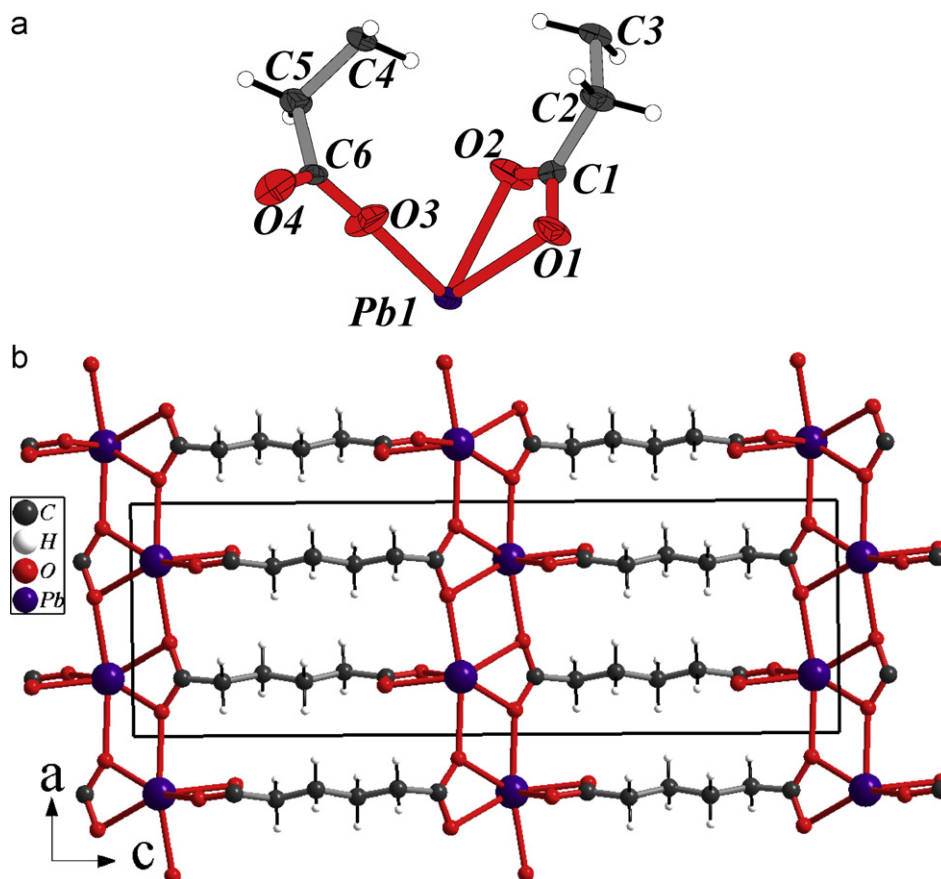


Fig. 2. (a) ORTEP plot of  $\text{Pb}(\text{C}_6\text{H}_8\text{O}_4)$ , **II** (thermal ellipsoids are shown at 50% probability), (b) the 3-D structure of **II** viewed along the  $b$ -axis.

seven-coordinated by oxygen atoms from two oxalate and three succinate anions. Six of the oxygens have  $\mu_3$  connections linking two different Pb atoms. This leads to a connectivity wherein each Pb atom is connected with four other Pb atoms. Thus, each  $\text{PbO}_7$  polyhedron shares four of its corners with four other  $\text{PbO}_7$  polyhedra forming an infinite 2-D Pb–O–Pb layer of the  $I^2O^0$  type, with a (4,4) net topology very similar to that in **III** (Fig. 4d). This layer can be viewed as chains of only corner shared  $\text{PbO}_7$  polyhedra and connected through the corners of  $\text{PbO}_7$  polyhedra in the adjacent chains. Two of these layers are connected to each other through the oxalate anions into a bilayer structure (Fig. 4e). These bilayers are further connected to each other through succinate anions into a 3-D structure of the  $I^2O^1$  type (Fig. 4e). The Pb–O bond lengths are in the 2.394–2.890 Å range.

The oxalate-adipate,  $\text{Pb}_2(\text{C}_2\text{O}_4)(\text{C}_6\text{H}_8\text{O}_4)$ , **V**, has a 3-D structure similar to **IV**, with an asymmetric unit of nine non-hydrogen atoms (Fig. 5a). The asymmetric unit contains a crystallographically distinct  $\text{Pb}^{2+}$  ion, one half of the oxalate and one half of the adipate anions. The oxalate and adipate anions exhibit coordination modes with (2222) and (1212) connectivities, respectively, both with  $0^\circ$  torsional angle (Figs. 4b and 5b). The Pb atom is holo-directed and seven-coordinated by oxygen atoms from two different oxalate and three different succinate anions. Six of the oxygens have  $\mu_3$  connections linking two

different Pb atoms, leading to a connectivity just as in **IV**, giving rise to an infinite 2-D Pb–O–Pb layer of the  $I^2O^0$  type, with a (4,4) net topology. The layers are connected to each other through the oxalate anions to form bilayers (Fig. 5c). The bilayers further get connected through adipate anions into a 3-D structure of the  $I^2O^1$  type (Fig. 5c). The Pb–O bond lengths are in the 2.402–2.867 Å range.

The 3-D lead aliphatic dicarboxylates, **I–III** (homoleptic) and **IV** and **V** (heteroleptic or mixed ligands) all possess infinite 2-D layers of the  $I^2O^0$  type which are connected by the dicarboxylate moiety. The inorganic layers can be further categorized in to two types: Type **A**: compounds **I–II** (Fig. 1c) and Type **B**: **III–V** (Figs. 3c and 4d). The difference between **A** and **B** arises from the different polyhedral connectivities in the inorganic layers. The origin of the difference can be attributed to the torsional angles of the dicarboxylate moieties. In type **A**, the torsional angles are close to  $100^\circ$ , whereas it is zero in type **B**. This observation gains support from the structures of other lead aliphatic dicarboxylates. Thus, lead azelate [35],  $\text{Pb}(\text{C}_9\text{H}_{14}\text{O}_4)$ , with a torsional angle of  $93.11^\circ$ , possesses **A** type inorganic layers connected by the azelate moieties. Lead succinate,  $\text{Pb}(\text{C}_4\text{H}_4\text{O}_4)$  [28], with a torsional angle of  $90.41^\circ$ , possesses M–O–M inorganic chains, closely related to the connectivity in **A** type layers. In lead succinates [28,36], the conformation of the acid plays a role in

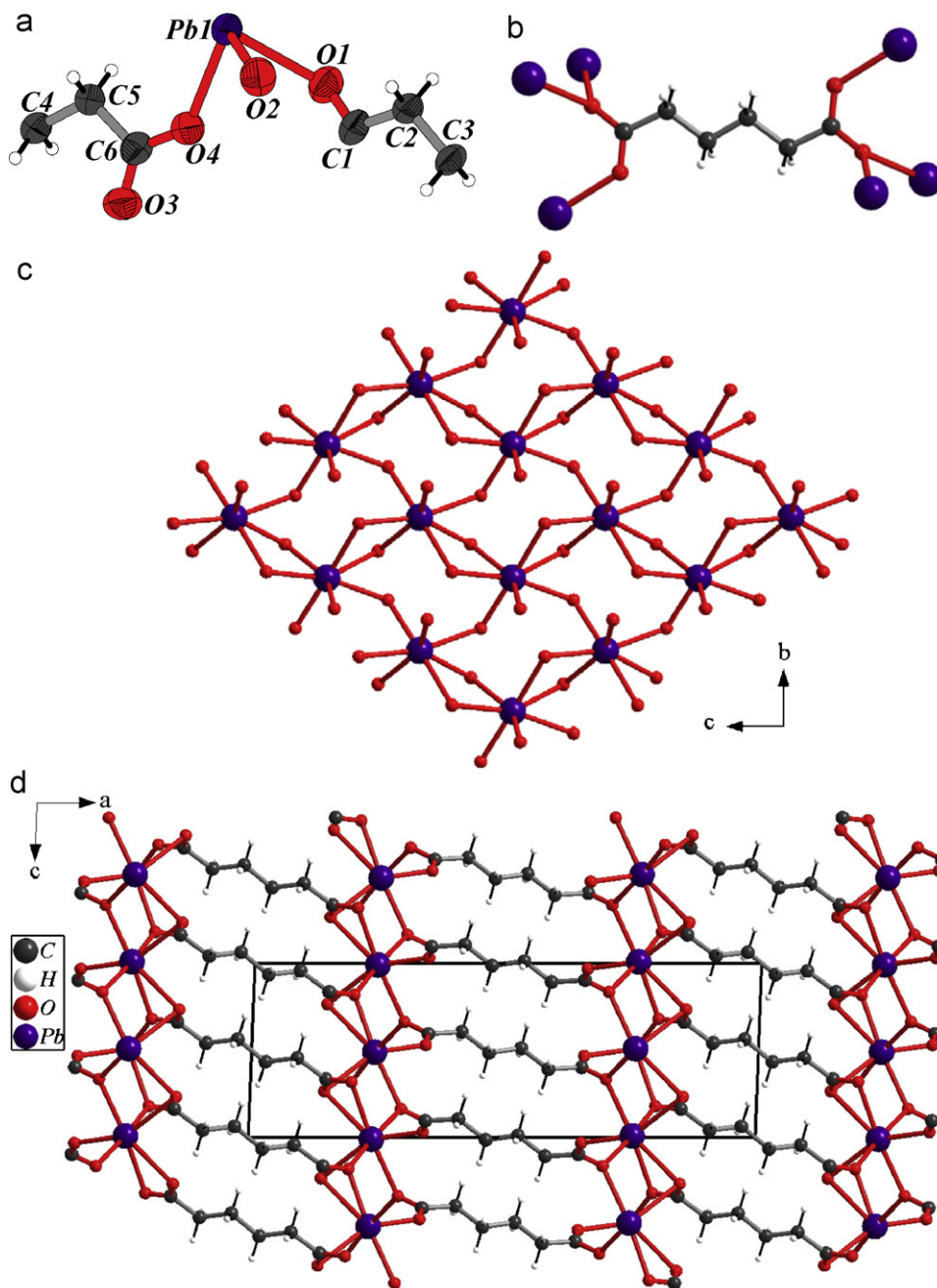


Fig. 3. (a) ORTEP plot of  $\text{Pb}(\text{C}_6\text{H}_8\text{O}_4)$ , **III** (thermal ellipsoids are shown at 50% probability), (b) coordination mode of the adipate moiety in **III**, (c) view of the inorganic layer with the infinite Pb–O–Pb linkages of the  $I^2O^0$  type in **III** and (d) the 3-D structure of **III** viewed along the  $b$ -axis.

determining the structure. In the lower dicarboxylates, such as malonates [37,38] and oxalates [39–41], the main factor is the coordination mode of the acid, coordination number (CN) and the geometry of lead cation, the torsional angle being always close to zero.

The heteroleptic 3-D compounds, **IV** (oxalate-succinate) and **V** (oxalate-adipate), possess a unique bilayer oxalate with the inorganic layer of the  $I^2O^1$  type (Fig. 4d) connected by the succinate or adipate anions into 3-D structures. The other known hybrid heteroleptic aliphatic dicarboxylates are neodymium oxalate-glutarate [25],  $\text{Nd}_4(\text{H}_2\text{O})_2(\text{C}_5\text{H}_6\text{O}_4)_4(\text{C}_2\text{O}_4)_2$ , lanthanum oxalate-suc-

nate [26],  $[\text{La}_2(\text{C}_2\text{O}_4)(\text{C}_4\text{H}_4\text{O}_4)_2(\text{H}_2\text{O})_4] \cdot 4\text{H}_2\text{O}$ , lanthanum oxalate-adipate [26],  $\text{La}_2(\text{C}_2\text{O}_4)_2(\text{C}_6\text{H}_8\text{O}_4)(\text{H}_2\text{O})_2$ , and lanthanide oxalate-fumarate [27],  $[\text{La}_2(\text{C}_2\text{O}_4)(\text{C}_4\text{H}_2\text{O}_4)_2(\text{H}_2\text{O})_4] \cdot 4\text{H}_2\text{O}$ , ( $L_n = \text{Eu}, \text{Tb}$ ). The first three are the 3-D compounds possessing one-dimensional (1-D)  $I^1O^0$  type M–O–M infinite chains. The oxalate-fumarate is a coordination polymer of the  $I^0O^3$  type where four member  $L_n$  clusters are connected by carboxylate moieties.

The oxalate-nitrate,  $(\text{OPb}_2)_2(\text{C}_2\text{O}_4)(\text{NO}_3)_2$ , **VI**, has a 2-D structure with an asymmetric unit of 10 atoms (Fig. 6a). There are two crystallographically distinct  $\text{Pb}^{2+}$  ions Pb(1) and Pb(2) in the asymmetric unit. One nitrate anion, one

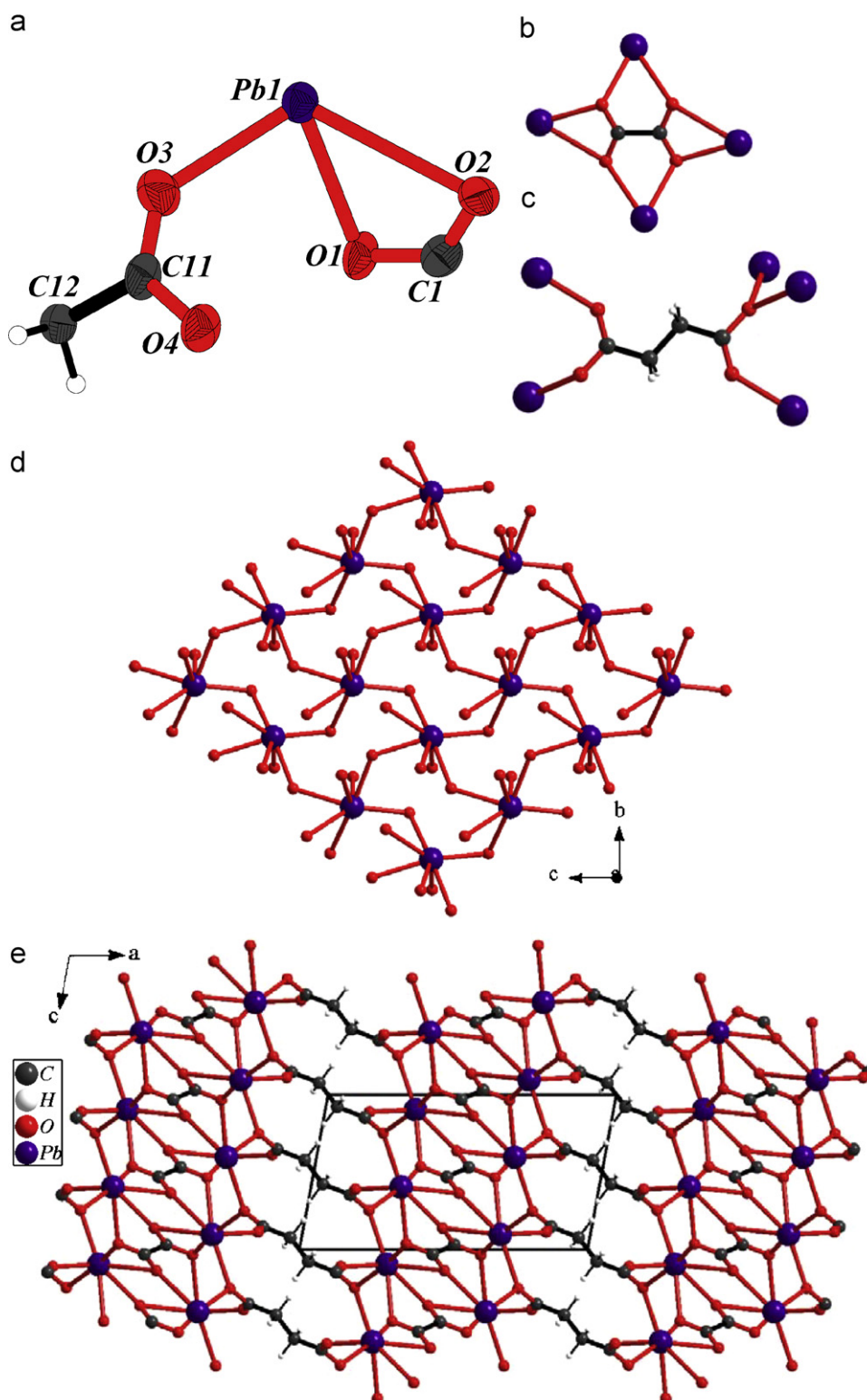


Fig. 4. (a) ORTEP plot of  $\text{Pb}_2(\text{C}_2\text{O}_4)(\text{C}_4\text{H}_4\text{O}_4)$ , **IV** (thermal ellipsoids are shown at 50% probability) (b) coordination mode of the oxalate moiety in **IV** (c) coordination mode of the succinate moiety in **IV** (d) view of the inorganic layer with the infinite Pb–O–Pb linkages of the  $\tilde{P}^2O^0$  type in **IV** and (e) the 3-D structure of **IV** viewed along the *b*-axis.

half of the oxalate anion and one independent oxo dianion are also in the asymmetric unit. The oxalate anion exhibits a coordination mode with (1221) connectivity with zero torsional angle and the planar nitrate anion is having (233)

connectivity (Fig. 6b). Pb(1) is hemi-directed and seven-coordinated by oxygen atoms ( $\text{PbO}_7$ ) from three different nitrate anions and an apical oxo dianion. Six of the oxygens have  $\mu_4$  connections linking Pb(1) with two other

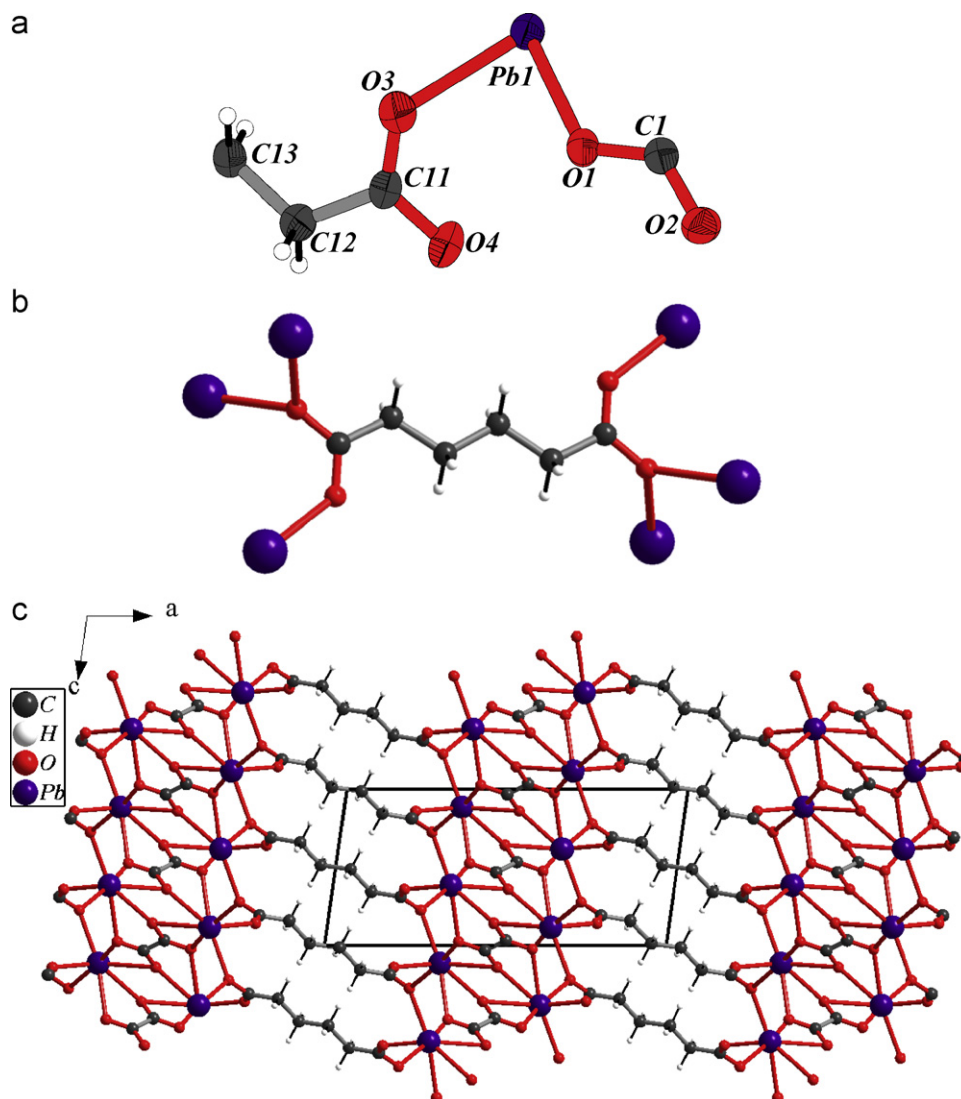


Fig. 5. (a) ORTEP plot of  $\text{Pb}_2(\text{C}_2\text{O}_4)(\text{C}_6\text{H}_8\text{O}_4)$ , V (thermal ellipsoids are shown at 50% probability), (b) coordination mode of the succinate moiety in V and (c) the 3D structure of V viewed along the  $b$ -axis.

Pb(1) atoms and one Pb(2) atom. Thus, a Pb(1) $\text{O}_7$  polyhedron shares its six corners with other Pb(1) $\text{O}_7$  polyhedra forming an infinite 2-D Pb–O–Pb layer of the  $I^2O^0$  type, with a (6,3) 2-D net topology (Fig. 6c). The oxo dianion has  $\mu_2$  connectivity and links each Pb(1) with a Pb(2) atom. Pb(2) is hemi-directed and six-coordinated by oxygen atoms (Pb $\text{O}_6$ ) from an oxo dianion, two different nitrate anions and two different oxalate anions. These oxygens have  $\mu_2$ ,  $\mu_4$  and  $\mu_3$  connections, respectively. Thus, each Pb(2) $\text{O}_6$  polyhedron is linked by the oxalate anion to two of the polyhedron by corner-sharing to give rise an infinite 1-D chain. The chains of Pb(2) $\text{O}_6$  polyhedra are further connected to the layers formed by Pb(1) $\text{O}_7$  units through oxo and nitrate anions, forming an infinite 2-D layer with Pb–O–Pb linkages (Fig. 7a). While the active lone pair electron of the Pb(1) projects out on one side of the layer, the other side is decorated with chains of hemi-directed Pb(2) $\text{O}_6$  polyhedra. The oxalate anions connecting

these layers through the Pb(2) atom, form a double layer structure with the lone pair of electrons projecting out from both the sides of the double layer (Fig. 7b). These layers are packed in a ...AAA... manner without any H-bonding interactions. The Pb–O bond lengths are in the 2.268–2.830 Å range.

The oxalate-nitrate, VI is a unique hybrid framework wherein infinite 2-D layers of lead nitrate of the  $I^2O^0$  type are connected by the oxalate moiety into a bilayer structure. Unlike the nitrate anion, oxy-anions such as phosphate, sulfate, sulfite and selenate are known to form organically templated inorganic framework compounds [42,43]. There are, however few organic inorganic hybrid compounds, wherein the nitrate anion is involved in the network formation [44–54]. Most of these compounds are with low-dimensional inorganic connectivity,  $I^m$  ( $m < 2$ ). The value of  $m$  depends on the nature of chelation, ligation number, coordination mode and connectivity of the nitrate



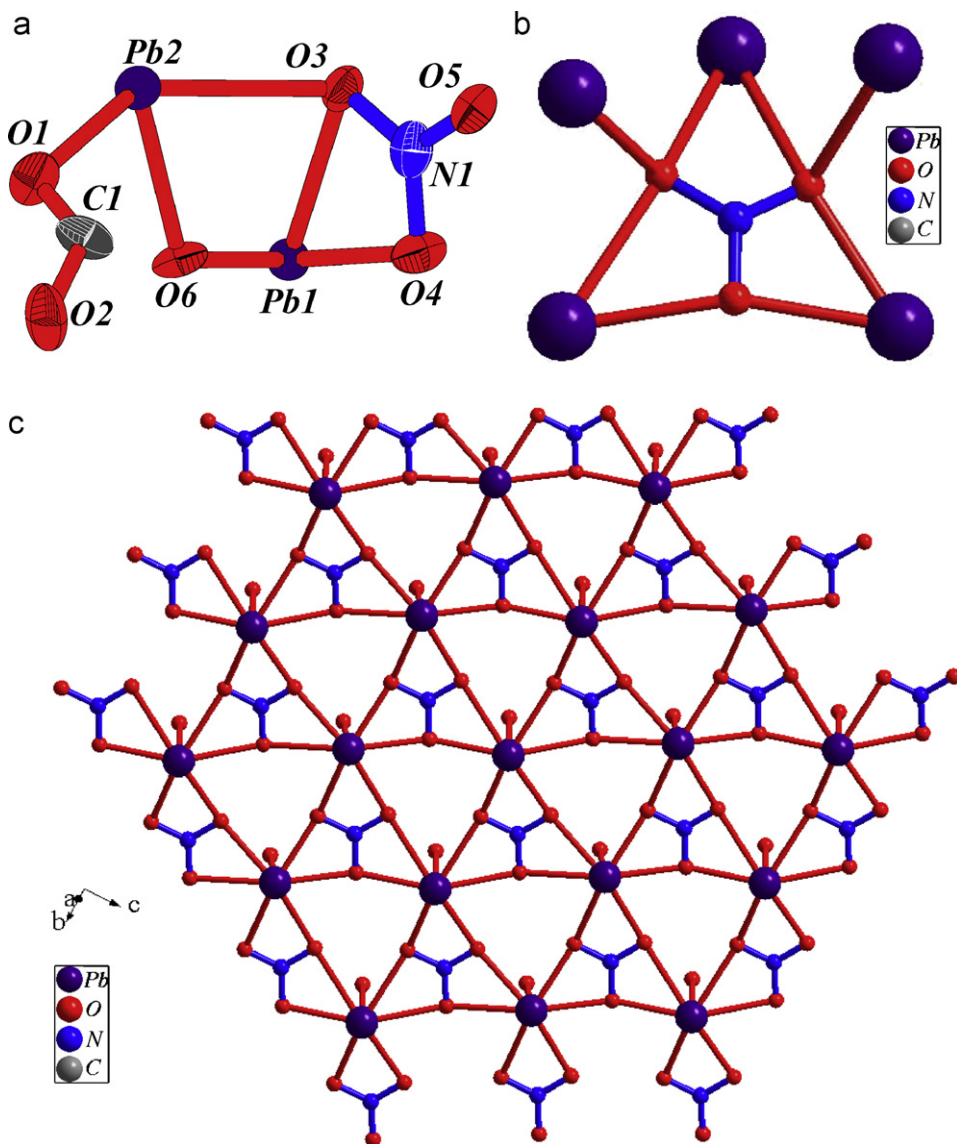


Fig. 6. (a) ORTEP plot of  $(\text{OPb}_2)_2(\text{C}_2\text{O}_4)(\text{NO}_3)_2$ , **VI** (thermal ellipsoids are shown at 50% probability), (b) coordination mode of the nitrate moiety in **VI** and (c) view of the inorganic layer with the infinite Pb–O–Pb linkages of the  $P^2O^0$  type in **VI**.

ions. The commonly observed connectivities in the low-dimensional hybrids are (110), (111), (112) and (122) with zero to two chelations per single nitrate moiety. The hybrid compound **VI** is appears to be only the second example after  $\text{Ag}(\text{C}_5\text{H}_5\text{NO})\text{NO}_3$  [54], possessing a 2-D inorganic metal nitrate layer with infinite M–O–M linkages. The connectivities of the nitrate in **VI** are unique with (233) connectivity with three chelations (Fig. 6b). In  $\text{Ag}(\text{C}_5\text{H}_5\text{NO})\text{NO}_3$ , the connectivity is (222) with three chelations.

The Pb(II) cations in **I–V** exhibit either hemi- and holo-directed geometry with a CN of 7. **I** and **II**, with type **A** inorganic layers possess Pb(II) cations in hemi-directed geometry with a CN of 7, whereas **III–V**, with type **B** inorganic layers possess Pb(II) cations in holo-directed geometry with a CN of 7. The 2-D compound, **VI**, with

a inorganic bilayer structure has Pb(II) cations in hemi-directed geometries with CN of 6 and 7 respectively. A situation has been reported in another Pb carboxylate where the Pb(II) cations are present with both hemi- and holo-directed geometries [24].

#### 4. Conclusions

In conclusion, we have synthesized and characterized five 3-D (**I–V**) and one 2-D (**VI**) hybrid lead dicarboxylates, all possessing 2-D inorganic connectivity. Of these two of them, the Pb glutarate, **I**, and adipate, **II**, possess one type of 2-D inorganic connectivity with near  $90^\circ$  torsional angle of the dicarboxylate anions and hemi-directed Pb(II) cations. The Pb adipate, **III**, as well as the oxalate-succinate, **IV**, and oxalate-adipate, **V**, possess another type

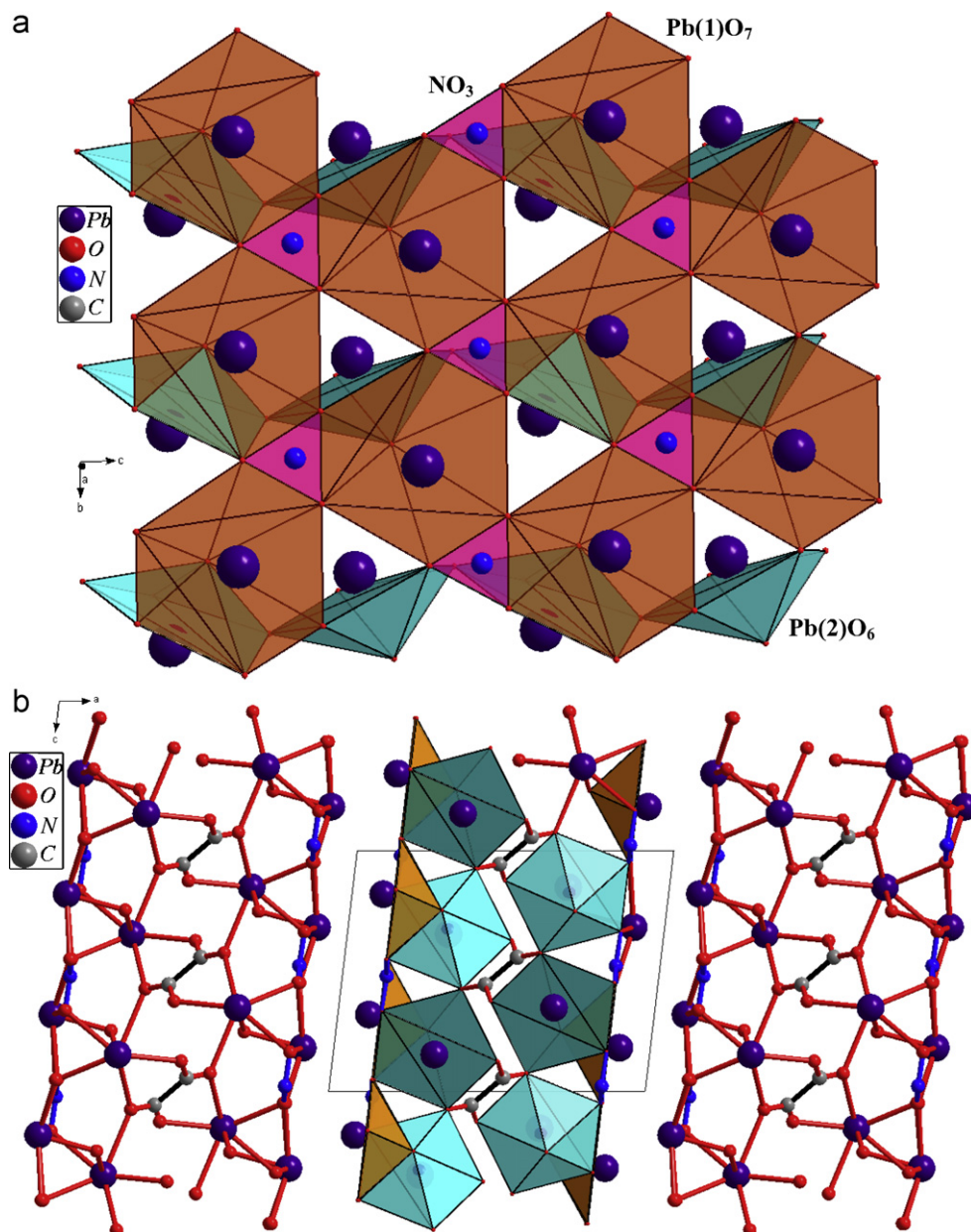


Fig. 7. (a) View of the inorganic layer with the infinite Pb–O–Pb linkages of the  $F^2O^0$  type in  $(\text{OPb}_2)_2(\text{C}_2\text{O}_4)(\text{NO}_3)_2$ , VI showing the polyhedral connectivity between  $\text{Pb(1)O}_7$  (orange),  $\text{Pb(2)O}_7$  (cyan) and  $\text{NO}_3$  (pink) moieties and (b) the packing arrangement in VI.

of 2-D inorganic connectivity with the dicarboxylate anions in the zero torsional angle and holo-directed Pb(II) cations. The bilayer nitrate-oxalate, VI, is unusual in that it possesses a (6,3) net topology of the 2-D inorganic metal nitrate layer, with infinite M–O–M linkages. The Pb(II) cations in VI are in hemi-directed geometry.

#### Supporting information available

Crystallographic data (excluding structure factors) for the structures (compounds I–VI) reported in this paper have been deposited with the Cambridge Crystallographic

Data Centre as supplementary publication numbers. CCDC 670598–670603. Copies of the data can be obtained free of charge on application to CCDC, 12 Union Road, Cambridge CB2 1EZ, UK (fax: +44 1223 336 033; e-mail: deposit@ccdc.cam.ac.uk).

#### Acknowledgment

AT thanks the Council of Scientific and Industrial Research (CSIR), Government of India, for the award of the Senior Research Fellowship and Dr. Sukhendu Mandal for his help in solving a crystal structure.

## Appendix A. Supplementary materials

Supplementary data associated with this article can be found in the online version at [doi:10.1016/j.jssc.2008.02.018](https://doi.org/10.1016/j.jssc.2008.02.018).

## References

- [1] C.N.R. Rao, S. Natarajan, R. Vaidyanathan, *Angew. Chem. Int. Ed.* 43 (2004) 1466–1496.
- [2] D. Maspoch, D. Ruiz-Molina, J. Veciana, *Chem. Soc. Rev.* 36 (2007) 770–818.
- [3] N. Guillou, C. Livage, G. Férey, *Eur. J. Inorg. Chem.* (2006) 4963–4978.
- [4] N.W. Ockwig, O. D-Friedrichs, M. O’Keeffe, O.M. Yaghi, *Acc. Chem. Res.* 38 (2005) 176–182.
- [5] N.L. Rosi, J. Eukert, M. Eddaoudi, D.T. Vodak, J. Kim, M. O’Keeffe, O.M. Yaghi, *Science* 300 (2003) 1127–1129.
- [6] G. Férey, C. Mellot-Draznieks, C. Serre, F. Millange, J. Dutour, S. Surblé, I. Margiolaki, *Science* 309 (2005) 2040–2042.
- [7] C. Serre, F. Millange, S. Surblé, G. Férey, *Angew. Chem. Int. Ed.* 43 (2004) 6285–6289.
- [8] L.-S. Long, X.-M. Chen, M.-L. Tong, Z.-G. Sun, Y.-P. Ren, R.-B. Huang, L.-S. Zheng, *J. Chem. Soc. Dalton Trans.* (2001) 2888–2890.
- [9] C. Livage, C. Egger, M. Nogués, G. Férey, *J. Mater. Chem.* 8 (1998) 2743–2747.
- [10] C. Livage, C. Egger, G. Férey, *Chem. Mater.* 11 (1999) 1546–1550.
- [11] N. Guillou, C. Livage, M. Drillon, G. Férey, *Angew. Chem. Int. Ed.* 42 (2003) 5314–5317.
- [12] P.M. Forster, A.K. Cheetham, *Angew. Chem. Int. Ed.* 41 (2002) 457–459.
- [13] R. Vaidyanathan, S. Natarajan, C.N.R. Rao, *Dalton Trans.* (2003) 1459–1464.
- [14] R. Vaidyanathan, S. Natarajan, C.N.R. Rao, *Cryst. Growth Des.* 3 (2003) 47–51.
- [15] S.C. Manna, E. Zangrando, A. Bencini, C. Benelli, N.R. Chaudhuri, *Inorg. Chem.* 45 (2006) 9114–9122.
- [16] S. Konar, P.S. Mukherjee, E. Zangrando, F. Lloret, N.R. Chaudhuri, *Angew. Chem. Int. Ed.* 41 (2002) 1561–1563.
- [17] A.K. Cheetham, C.N.R. Rao, R.K. Feller, *Chem. Commun.* (2006) 4780–4795.
- [18] M. Kurmoo, H. Kumagai, S.M. Hughes, C.J. Kepert, *Inorg. Chem.* 42 (2003) 6709–6722.
- [19] Z.-L. Huang, M. Drillon, N. Masciocchi, A. Sironi, J.-T. Zhao, P. Rabu, P. Panissod, *Chem. Mater.* 12 (2000) 2805–2812.
- [20] K. Barthelet, K. Adil, F. Millange, C. Serre, D. Riou, G. Férey, *J. Mater. Chem.* 13 (2003) 2208–2212.
- [21] C.A. Merrill, A.K. Cheetham, *Inorg. Chem.* 46 (2007) 278–284.
- [22] A. Thirumurugan, M.B. Avinash, C.N.R. Rao, *Dalton Trans.* (2006) 221–228.
- [23] K.P. Rao, A. Thirumurugan, C.N.R. Rao, *Chem. Eur. J.* 13 (2007) 3193–3201.
- [24] A. Thirumurugan, R. Sanguramath, C.N.R. Rao, *Inorg. Chem.* 47 (2008) 823–831.
- [25] R. Vaidyanathan, S. Natarajan, C.N.R. Rao, *J. Solid State Chem.* 177 (2004) 1444–1448.
- [26] M. Dan, G. Cottureau, C.N.R. Rao, *Solid State Sci.* 7 (2005) 437–443.
- [27] W.-H. Zhu, Z.-M. Wang, S. Gao, *Inorg. Chem.* 46 (2007) 1337–1342.
- [28] M.R. St J. Foreman, M.J. Plater, J.M.S. Skakle, *J. Chem. Soc. Dalton Trans.* (2001) 1897–1903.
- [29] S. Barbara, *Infrared Spectroscopy: Fundamentals and Applications*, Wiley, New York, 2004.
- [30] R.M. Silverstein, G.C. Bassler, T.C. Morrill, *Spectrometric Identification of Organic Compounds*, Wiley, New York, 1963.
- [31] K. Nakamoto, *Infrared and Raman Spectra of Inorganic and Coordination Compounds*, Wiley, New York, 1978.
- [32] G.M. Sheldrick, SADABS Siemens Area Detector Absorption Correction Program, University of Göttingen, Göttingen, Germany, 1994.
- [33] G.M. Sheldrick, SHELXTL-PLUS Program for Crystal Structure Solution and Refinement, University of Göttingen, Göttingen, Germany, 1997.
- [34] D. Massiot, S. Drumel, P. Janvier, M. B-Doeuff, B. Bujoli, *Chem. Mater.* 9 (1997) 6–7.
- [35] M.J. Plater, B. De Silva, T. Gelbrich, M.B. Hursthouse, C.L. Higgitt, D.R. Saunders, *Polyhedron* 22 (2003) 3171–3179.
- [36] K. Nagase, H. Yokobayashi, *Chem. Lett.* (1974) 861–864.
- [37] J.R. Gunter, *Cryst. Res. Technol.* 17 (1982) K123–K125.
- [38] W. Bensch, J.R. Gunter, *Z. Kristallogr.* 178 (1987) 257–262.
- [39] A.V. Virovets, D.Yu. Naumov, E.V. Boldyreva, N.V. Podberezskaya, *Acta Crystallogr. Sect. C: Cryst. Struct. Commun.* 49 (1993) 1882–1884.
- [40] H. S-Hua, W. Ru-Ji, T.C.W. Mak, *J. Crystallogr. Spectrosc. Res.* 20 (1990) 99–104.
- [41] A.N. Christensen, D. Cox, M.S.E. Lehmann, *Acta Chem. Scand.* 43 (1989) 19–25.
- [42] A.K. Cheetham, G. Férey, T. Loiseau, *Angew. Chem. Int. Ed.* 38 (1999) 3268–3292.
- [43] C.N.R. Rao, J.N. Behera, M. Dan, *Chem. Soc. Rev.* 35 (2006) 375–387.
- [44] B.G. Cooksey, L.T. Gibson, A.R. Kennedy, D. Littlejohn, L. Stewart, N.H. Tennent, *Acta Crystallogr., Sect. C: Cryst. Struct. Commun.* 55 (1999) 324–326.
- [45] L. Zhao, T.C.W. Mak, *J. Am. Chem. Soc.* 126 (2004) 6852–6853.
- [46] J.-P. Costes, F. Dahan, A. Dupuis, J.-P. Laurent, *Inorg. Chem.* 39 (2000) 169–173.
- [47] Y.-Q. Zheng, J.-L. Lin, W.-J. Chen, *Z. Kristallogr. New Cryst. Struct.* 216 (2001) 269–270.
- [48] C.L. Lengauer, G. Giester, *Acta Crystallogr. Sect. C: Cryst. Struct. Commun.* 53 (1997) 870–872.
- [49] M. Fangming, L. Xiaolan, Z. Shufen, J. Zonghui, W. Genglin, Wuli Huaxue Xuebao (*Acta Phys. Chim. Sin.*) 4 (1988) 20–26 (in Chinese).
- [50] K. Lashgari, M. Kritikos, K. Lashgari, G. Westin, *Acta Crystallogr. Sect. C: Cryst. Struct. Commun.* 54 (1998) 1794–1797.
- [51] G.A. Bowmaker, B. Assadollahzadeh, A.M. Brodie, E.W. Ainscough, G.H. Freeman, G.B. Jameson, *Dalton Trans.* (2005) 1602–1612.
- [52] M. Hashimoto, M. Takata, A. Yagasaki, *Inorg. Chem.* 39 (2000) 3712–3714.
- [53] G.A. Bowmaker, Effendy, S. Marfua, B.W. Skelton, A.H. White, *Inorg. Chim. Acta* 358 (2005) 4371–4388.
- [54] G.A. Bowmaker, Effendy, M. Nitiatmodjo, B.W. Skelton, A.H. White, *Inorg. Chim. Acta* 358 (2005) 4327–4341.